

AD-A179 983

## Saturation of Response of PbS Infrared Detectors Under High Flux

Prepared by  
A. A. FOTE  
Laboratory Operations  
The Aerospace Corporation  
El Segundo, CA 90245

10 April 1987

Prepared for  
SPACE DIVISION  
AIR FORCE SYSTEMS COMMAND  
Los Angeles Air Force Station  
P.O. Box 92960, Worldway Postal Center  
Los Angeles, CA 90009-2960

DTIC  
ELECTE  
MAY 04 1987  
S \* E D

APPROVED FOR PUBLIC RELEASE  
DISTRIBUTION UNLIMITED

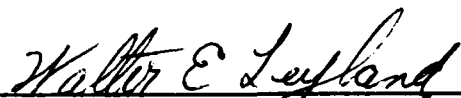
87 5 1 004

**BLANK PAGES  
IN THIS  
DOCUMENT  
WERE NOT  
FILMED**

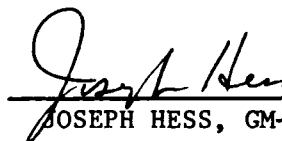
This report was submitted by The Aerospace Corporation, El Segundo, CA 90245, under Contract No. F04701-85-C-0086-P00016 with the Space Division, P.O. Box 92960, Worldway Postal Center, Los Angeles, CA 90009-2960. It was reviewed and approved for The Aerospace Corporation by S. Feuerstein, Director, Chemistry and Physics Laboratory. Lt. Walter E. Leyland SD/CNDA was the Air Force project officer.

This report has been reviewed by the Public Affairs Office (PAS) and is releasable to the National Technical Information Service (NTIS). At NTIS, it will be available to the general public, including foreign nationals.

This technical report has been reviewed and is approved for publication. Publication of this report does not constitute Air Force approval of the report's findings or conclusions. It is published only for the exchange and stimulation of ideas.



WALTER E. LEYLAND, Lt, USAF  
MOIE Project Officer  
SD/CNDA



JOSEPH HESS, GM-15  
Director, AFSTC West Coast Office  
AFSTC/WCO OL-AB

UNCLASSIFIED

SECURITY CLASSIFICATION OF THIS PAGE (When Data Entered)

REPORT DOCUMENTATION PAGE		READ INSTRUCTIONS BEFORE COMPLETING FORM	
1. REPORT NUMBER SD-TR-87-16	2. GOVT ACCESSION NO. <b>A DA179983</b>	3. RECIPIENT'S CATALOG NUMBER	
4. TITLE (and Subtitle)  SATURATION OF RESPONSE OF PbS INFRARED DETECTORS UNDER HIGH FLUX		5. TYPE OF REPORT & PERIOD COVERED	
		6. PERFORMING ORG. REPORT NUMBER TR-0085A(5409-11)-1	
7. AUTHOR(s)  Alfred A. Fote		8. CONTRACT OR GRANT NUMBER(s)  F04701-85-C-0086-P00016	
9. PERFORMING ORGANIZATION NAME AND ADDRESS The Aerospace Corporation El Segundo, CA 90245		10. PROGRAM ELEMENT, PROJECT, TASK AREA & WORK UNIT NUMBERS	
11. CONTROLLING OFFICE NAME AND ADDRESS		12. REPORT DATE 10 April 1987	
		13. NUMBER OF PAGES 16	
14. MONITORING AGENCY NAME & ADDRESS (if different from Controlling Office) Space Division Los Angeles Air Force Station Los Angeles, CA 90009-2960		15. SECURITY CLASS. (of this report) Unclassified	
		15a. DECLASSIFICATION/DOWNGRADING SCHEDULE	
16. DISTRIBUTION STATEMENT (of this Report)  Approved for public release: distribution unlimited.			
17. DISTRIBUTION STATEMENT (of the abstract entered in Block 20, if different from Report)			
18. SUPPLEMENTARY NOTES			
19. KEY WORDS (Continue on reverse side if necessary and identify by block number)  PbS infrared detectors, <i>lab. results</i> incident flux chopped radiation, <i>etc.</i>			
20. ABSTRACT (Continue on reverse side if necessary and identify by block number)  Laboratory and mathematical results are provided to show that chopped radiation is approximately twice as effective as steady background radiation in causing saturation of PbS infrared detector performance at high flux levels.			

DD FORM 1473  
(IFACSIMILE)UNCLASSIFIED  
SECURITY CLASSIFICATION OF THIS PAGE (When Data Entered)

# CONTENTS

I.	INTRODUCTION.....	3
II.	EXPERIMENTAL SETUP.....	5
III.	RESULTS.....	7
IV.	ANALYSIS.....	13
V.	CONCLUSION.....	17

Accession For		
NTIS	GRA&I	<input checked="" type="checkbox"/>
DTIC	TAB	<input type="checkbox"/>
Unannounced		<input type="checkbox"/>
Justification		
By		
Distribution/		
Availability Codes		
Dist	Avail and/or Special	
A-1		



## I. INTRODUCTION

The responsivity of PbS infrared detectors will saturate under sufficiently high levels of incident flux. This flux can consist entirely of chopped radiation, as with a very strong signal. Alternately, it can include both a low intensity chopped radiation and an unchopped background. Whether or not these two types of flux lead to the same degree of saturation is not immediately apparent. If so, an unchopped background radiation could be simulated by increasing the signal flux to an equivalent level, taking into account the fact that approximately half of the radiation would be intercepted by the chopper blades in the latter. This study addresses that possibility.

## II. EXPERIMENTAL SETUP

Figure 1 depicts the experimental arrangement. The detector was mounted in a sorption-pumped vacuum chamber at the base of a liquid nitrogen dewar. A heater and an automatic temperature controller maintained the temperature of the detector to within 0.5 degrees C. A cold filter directly in front of the detector passed radiation only in the 2.66-2.78 micron band with a transmission coefficient of 0.5.

For responsivity measurements, the detector output, due to the chopped infrared radiation, was amplified with a current amplifier having a gain of  $2 \times 10^7$  V/A. A lock-in amplifier demodulated the signal and passed it on to a digital voltmeter. For the largest flux levels, it became necessary to interpose a ten-to-one voltage divider between the two amplifiers.

Two black bodies, each with their own choppers, acted as sources for infrared radiation. In order to reach the high flux levels required for this study, both black bodies were set at 900 degrees C. A beam splitter allowed the detector to see both sources simultaneously. The transmission coefficient of the beam splitter was measured in situ as 0.74.

The flux due to black body #1 was calculated in the usual way, taking into account the transmissions of the filter and beam splitter, the distance between source and detector, and the form factor of the chopper. The flux from black body #2 was determined by comparing the relative strengths of the detector response resulting from each of the two sources individually. Care was taken to perform this comparison at low flux levels where the detector response was linear.

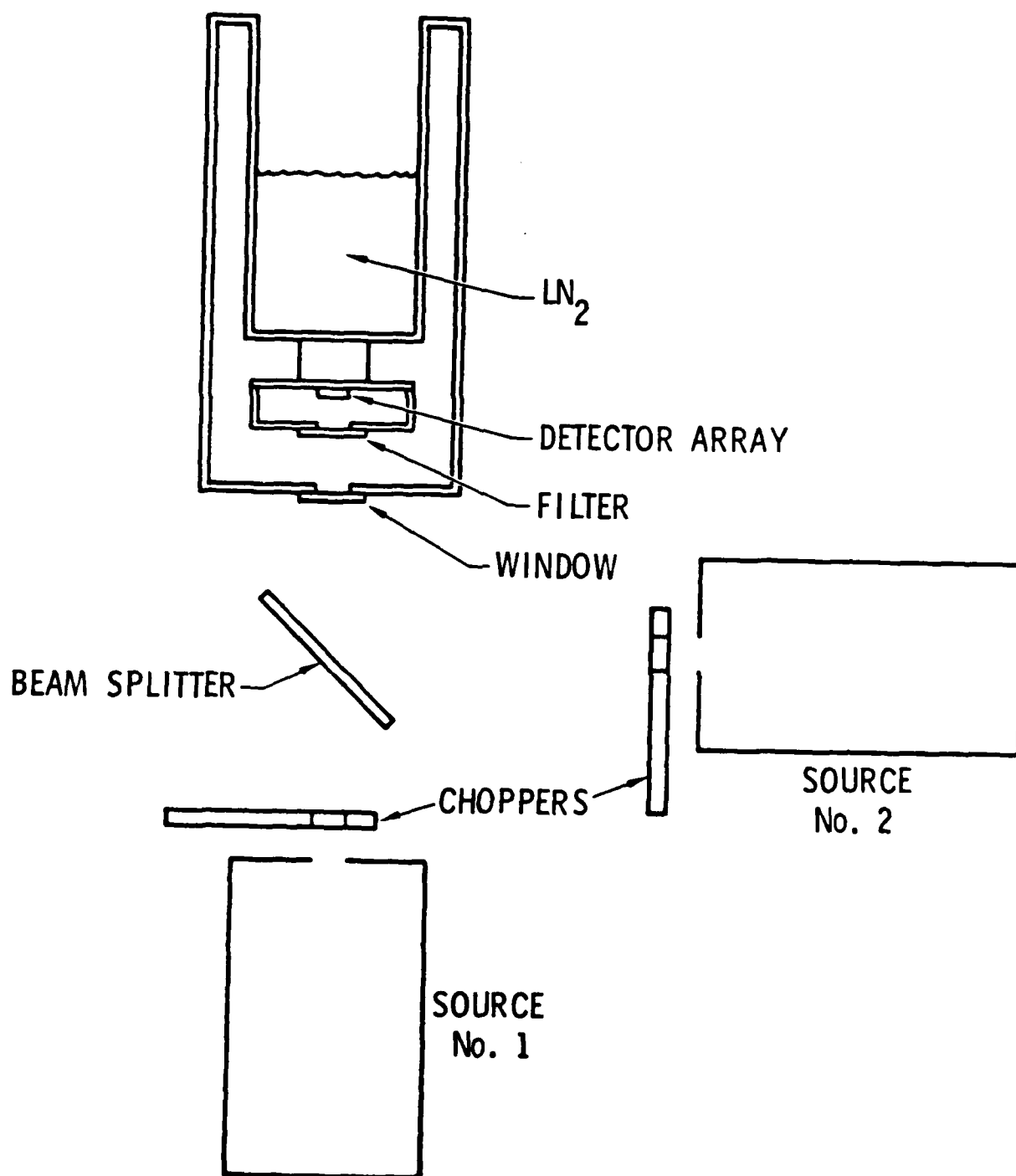


Figure 1. Experimental Setup



### III. RESULTS

The plots of Figures 2-4 summarize the results. Measurements of responsivity were taken at a detector temperature of 140°K and at frequencies of 16 Hz, 50 Hz, and 98 Hz. Each run consisted of two groups of data. First, source #2 was blocked and the response of the detector to chopped radiation from source #1 was measured as a function of flux level. The plots of these data are labeled "Zero background." Second, the response of the detector to chopped radiation from source #2 was measured under conditions of simultaneous illumination with unchopped radiation from source #1. These plots are labeled "with background". Two "with background" runs are included in Figures 2 and 4.) The leftmost data point of the "with background" plots were measured with source #1 blocked, that is, with no background.

In the first case, the "total flux" of the x-axis is given by

$$F = (1.049 \text{ E-4}) * B * A_1^2$$

where F is in Watts per sq. cm.; B is the transmission coefficient of the beam splitter; and  $A_1$  is the diameter, in inches, of the aperture of source #1. The numerical factor includes the effects of the source temperature, the source-detector distance, the chopper form-factor, and the transmission of the cold filter. The responsivity was calculated using

$$R = V / (32.54 * D * B * A_1^2)$$

where R is in Amps/Watt; V is the lock-in amplifier reading in mV; and D is the voltage divider factor, either 1.0 or 0.0893. The numerical factor includes the strength of the signal flux and the area of the detector.

In the second case, the "total flux" is

$$F = (1.049 \text{ E-4}) (2 * B * A_1^2 + A_2^2 / f)$$

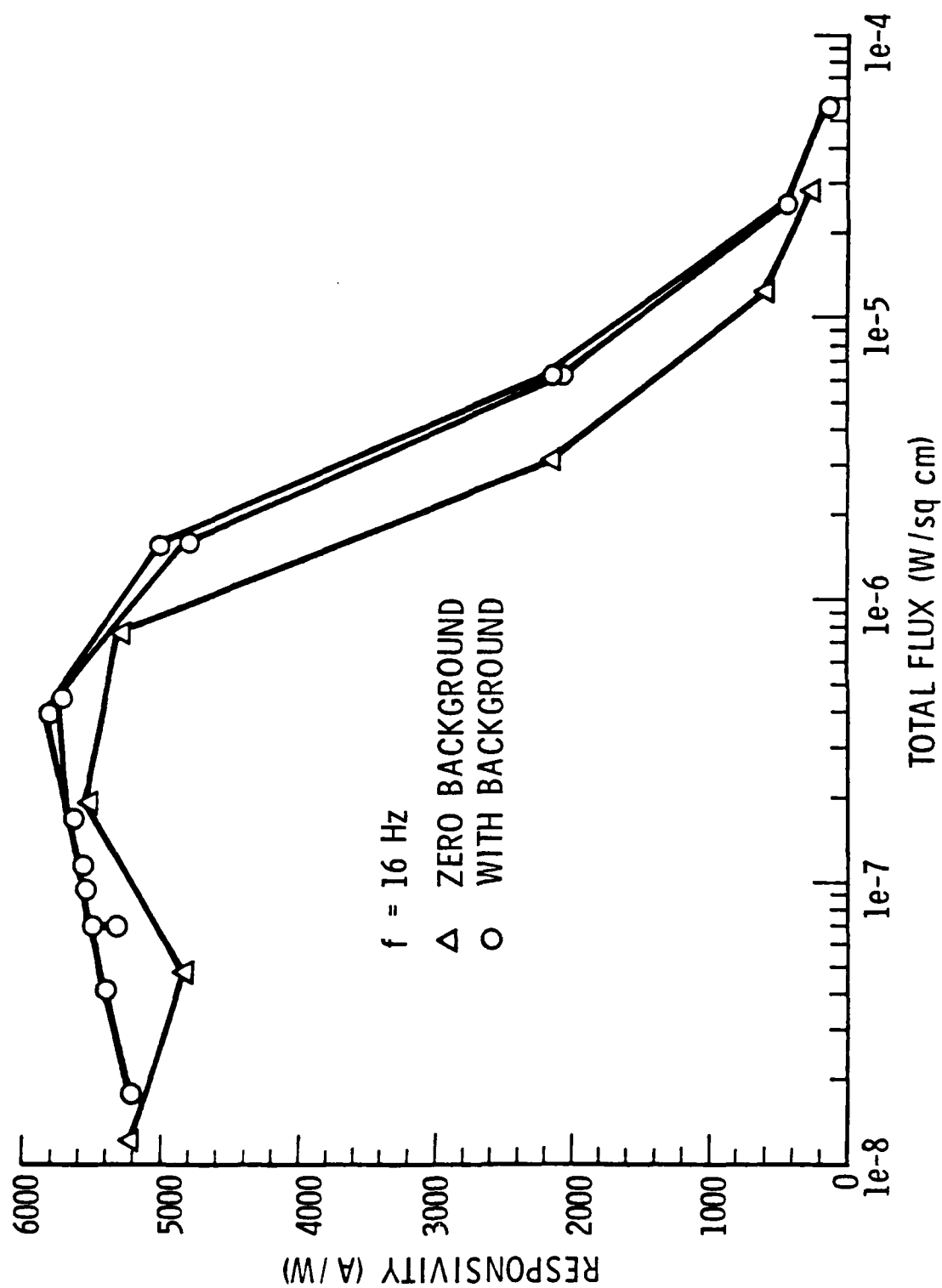


Figure 2. Responsivity vs. Total Flux (Signal Plus Background), 16 Hz

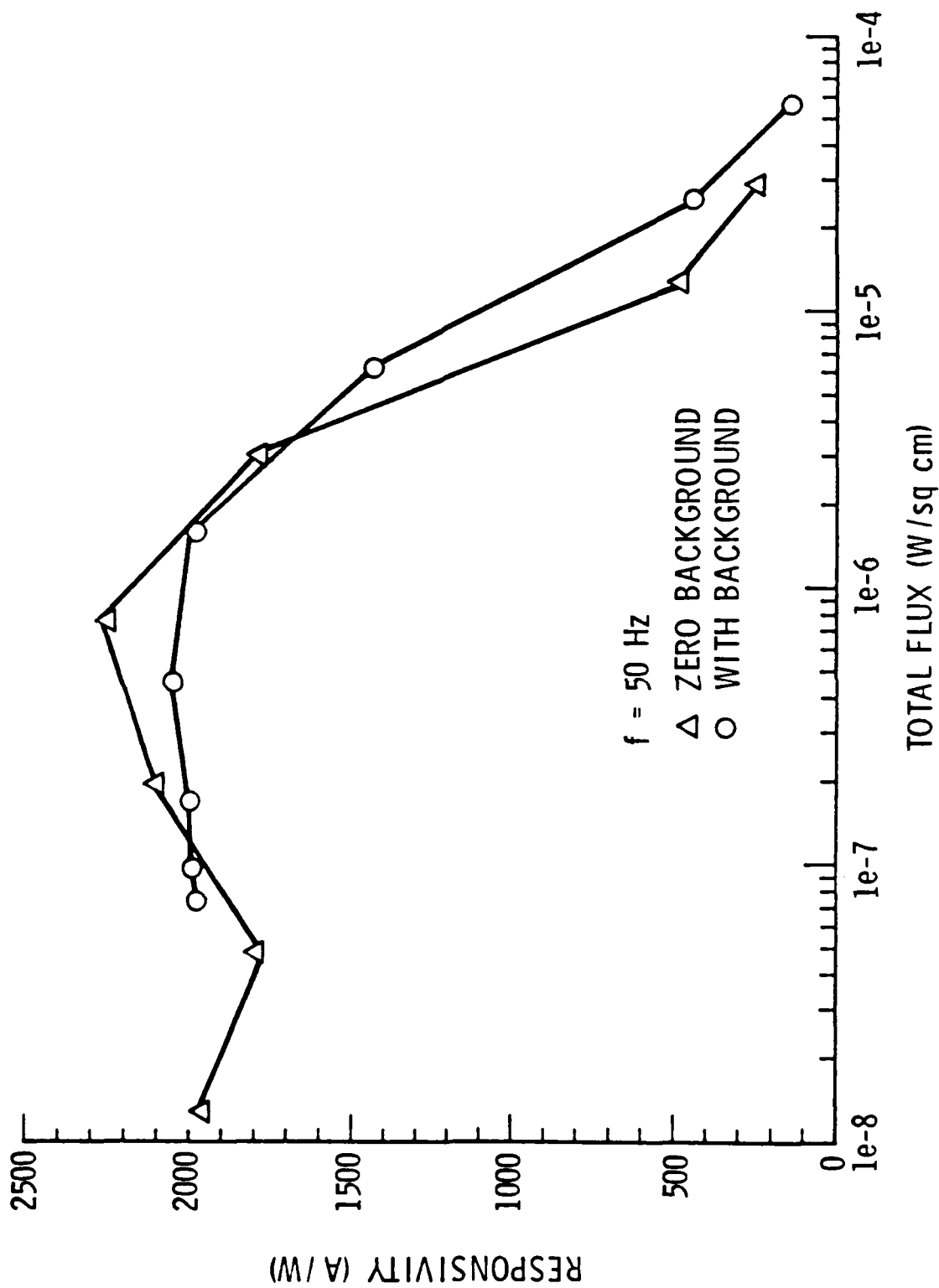


Figure 3. Responsivity vs. Total Flux (Signal Plus Background), 50 Hz

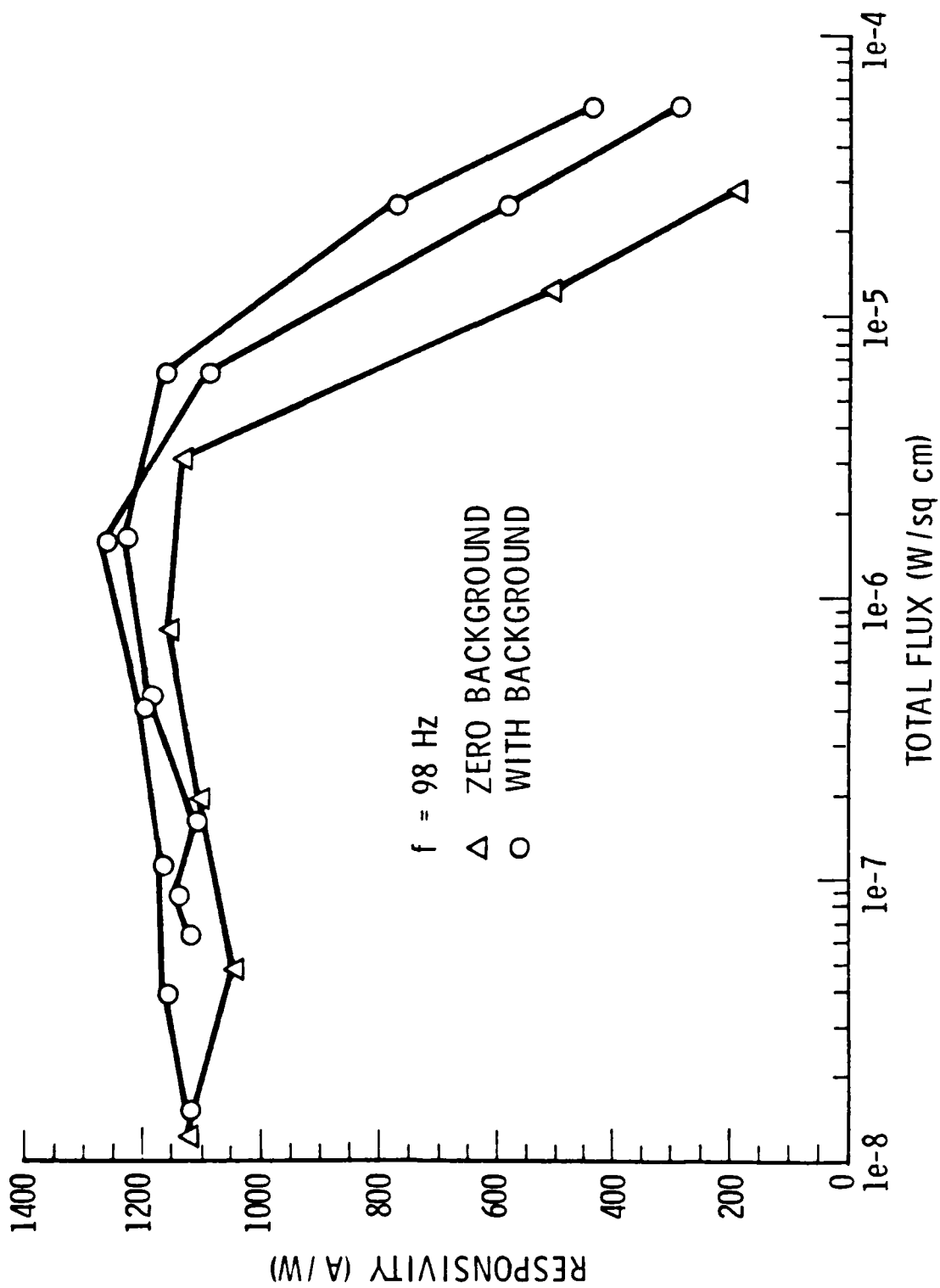


Figure 4. Responsivity vs. Total Flux (Signal Plus Background), 98 Hz

where the factor of 2 accounts for the fact that the radiation from source #1 is unchopped; A2 is the diameter, in inches, of the aperture of source #2; and f includes the effects of the different distances of the detector from the two sources and the reflection coefficient of the beam splitter. "f" was determined from the condition that the responsivity, as calculated under low level flux conditions from the equation

$$R = f \cdot V / (32.54 \cdot A_2^2),$$

should be the same as that measured when source #1 was used.

#### IV. ANALYSIS

The results of these measurements indicated that the chopped radiation was approximately twice as effective as steady background radiation in causing a saturation of detector performance at high flux levels. This can be explained as follows.

When infrared radiation strikes PbS, an electron-hole pair is created. The electron becomes immobilized in a "trap," presumably at a grain boundary, for an average lifetime,  $\tau$ . During that time, the mobile hole produces a signal in the form of an enhanced conductivity. Once the electron escapes from the trap and recombines with the hole, the signal decays. The responsivity is directly proportional to the lifetime,  $\tau$ .

The electron traps have a range of lifetimes. Larger binding energies correspond to longer lifetimes. At greater flux levels, the longer lifetime traps become full and additional photogenerated electrons occupy shorter lifetime traps. As a result, the average lifetime, and the responsivity, fall with increasing flux.

Both the background and the signal flux generate the same average number of electron-hole pairs, and therefore fill up the same number of traps on average. However, the average number of filled traps is not the important parameter. Rather, it is the number of traps that are filled during the dwell time,  $\tau_D$ , the half of every cycle when a chopper blade does not block the radiation. Traps filled during the remainder of the cycle do not affect the responsivity.

If the lifetime of the carriers,  $\tau$ , is much longer than  $\tau_D$ , the variations in the number of filled traps becomes averaged out to a constant level. Under that circumstance, the chopped radiation will be equally effective as the background in causing saturation. However, if  $\tau$  is short compared to  $\tau_D$ , the chopped flux will be approximately twice as effective at filling traps during the critical half cycle as will be the background flux. We will demonstrate this mathematically.

For the general case, we can determine the form factor,  $F$ , defined as the ratio between the effective flux and the equivalent background flux, as follows. We begin with the differential equation describing the number,  $N(t)$ , of free photogenerated carriers vs time.

$$dN(t)/dt = K*I(t) - N(t)/\tau$$

where  $I(t)$  represents the incident flux and  $K$  is a constant. For radiation chopped into a square wave, we have

$$I(t) = I, \quad t = 0 - \tau_D$$

$$I(t) = 0, \quad t = \tau_D - 2*\tau_D$$

This gives for  $N(t)$

$$N(t) = B*\exp(-t/\tau) + K*I*\tau, \quad t = 0 - \tau_D$$

$$N(t) = A*\exp(-t/\tau), \quad t = \tau_D - 2*\tau_D$$

The above equations can be solved for  $A$  and  $B$  by equating the two expressions at the boundaries  $t = 0$ ,  $\tau_D$ , and  $2*\tau_D$ . This gives for  $B$

$$B = K*I*\tau*(1-\exp X)/(2*\sinh X)$$

where  $X = \tau_D/\tau$ .

The average number of photogenerated carriers present during illumination,  $t = 0 - \tau_D$  is given by

$$\text{avg}(N) = \frac{1}{\tau_D} \int_0^{\tau_D} N(t)*dt$$

or

$$\text{avg}(N) = B*(1-\exp(-X))/X + K*I*\tau$$

We wish to compare the value of  $\text{avg}(N)$  due to chopped radiation,  $\text{avg}(N)_C$ , with that arising from steady background radiation,  $\text{avg}(N)_B$ , for the same total amount of radiation  $R$  actually falling on the detector. For the former case,  $R = I/2$ . For the latter case, we use  $dN(t)/dt = 0$  and  $I(t) = R$  in our differential equation to get

$$\text{avg}(N)_B = K*R*\tau$$

Defining the factor  $F$  by

$$F = \text{avg}(N)_C / \text{avg}(N)_B$$

finally gives

$$F = 2*((1-\cosh X)/(X*\sinh X) + 1).$$

Thus, it is easy to see that  $F = 1$  for very small values of  $X$  and  $F = 2$  for very large values of  $X$ .

The following formula describes the dependence of the lifetime of PbS photogenerated carriers as a function of flux level.

$$\tau = \tau_0 / (1 + 1.1E8*\tau_0*I)$$

where  $\tau_0 = 0.1$  sec. From this expression, we see that the lifetime falls below the inverse chopping frequency of  $1/16$  sec at  $I = 1E-6$ . Our data at 16 Hz confirms that the saturation of response becomes noticeable at and above that flux level. At the higher chopping frequencies, the initiation of saturation shifts to higher flux levels, again in agreement with the above equation.

Thus, the two effects are linked. At flux levels sufficiently high for saturation to occur,  $\tau$  will be short compared to  $\tau_D$  giving large  $X$  and



$F = 2$ . Under those conditions, the chopped signal flux will always be twice as efficient at filling traps during the critical half cycle than is the background flux.

## V. CONCLUSION

Signal flux can be used to simulate background flux provided that the detector lifetime and dwell time are taken into consideration. When  $\tau$  is less than  $\tau_D$ , this requires the inclusion of a factor of two when calculating the equivalent background radiation.

## LABORATORY OPERATIONS

The Aerospace Corporation functions as an "architect-engineer" for national security projects, specializing in advanced military space systems. Providing research support, the corporation's Laboratory Operations conducts experimental and theoretical investigations that focus on the application of scientific and technical advances to such systems. Vital to the success of these investigations is the technical staff's wide-ranging expertise and its ability to stay current with new developments. This expertise is enhanced by a research program aimed at dealing with the many problems associated with rapidly evolving space systems. Contributing their capabilities to the research effort are these individual laboratories:

Aerophysics Laboratory: Launch vehicle and reentry fluid mechanics, heat transfer and flight dynamics; chemical and electric propulsion, propellant chemistry, chemical dynamics, environmental chemistry, trace detection; spacecraft structural mechanics, contamination, thermal and structural control; high temperature thermomechanics, gas kinetics and radiation; cw and pulsed chemical and excimer laser development including chemical kinetics, spectroscopy, optical resonators, beam control, atmospheric propagation, laser effects and countermeasures.

Chemistry and Physics Laboratory: Atmospheric chemical reactions, atmospheric optics, light scattering, state-specific chemical reactions and radiative signatures of missile plumes, sensor out-of-field-of-view rejection, applied laser spectroscopy, laser chemistry, laser optoelectronics, solar cell physics, battery electrochemistry, space vacuum and radiation effects on materials, lubrication and surface phenomena, thermionic emission, photo-sensitive materials and detectors, atomic frequency standards, and environmental chemistry.

Computer Science Laboratory: Program verification, program translation, performance-sensitive system design, distributed architectures for spaceborne computers, fault-tolerant computer systems, artificial intelligence, micro-electronics applications, communication protocols, and computer security.

Electronics Research Laboratory: Microelectronics, solid-state device physics, compound semiconductors, radiation hardening; electro-optics, quantum electronics, solid-state lasers, optical propagation and communications; microwave semiconductor devices, microwave/millimeter wave measurements, diagnostics and radiometry, microwave/millimeter wave thermionic devices; atomic time and frequency standards; antennas, rf systems, electromagnetic propagation phenomena, space communication systems.

Materials Sciences Laboratory: Development of new materials: metals, alloys, ceramics, polymers and their composites, and new forms of carbon; non-destructive evaluation, component failure analysis and reliability; fracture mechanics and stress corrosion; analysis and evaluation of materials at cryogenic and elevated temperatures as well as in space and enemy-induced environments.

Space Sciences Laboratory: Magnetospheric, auroral and cosmic ray physics, wave-particle interactions, magnetospheric plasma waves; atmospheric and ionospheric physics, density and composition of the upper atmosphere, remote sensing using atmospheric radiation; solar physics, infrared astronomy, infrared signature analysis; effects of solar activity, magnetic storms and nuclear explosions on the earth's atmosphere, ionosphere and magnetosphere; effects of electromagnetic and particulate radiations on space systems; space instrumentation.